Article

Incident Velocity Induced Nonmonotonic Aging of Vapor-Deposited Polymer Glasses

Yuchu Wang and Yue Fan*

Read Online

ACCESS | Metrics & More | Article Recommendations | SI Supporting Information

ABSTRACT: Physical vapor deposition can produce remarkably stable glassy materials. However, a mechanistic understanding of the interplay between control parameters during such nonequilibrium processing (e.g., deposition rate, substrate temperature, incident velocity, etc.) remains an unresolved challenge to date. In this study, we report on the discovery of a dual role of incident molecules' mass-center velocity in controlling the stability of vapor-deposited glasses through atomistic modeling. On one hand, larger velocities would impose the surface atoms into a higher effective temperature environment and facilitate the relaxation as the sample approaches the glass transition temperature. On the other hand, larger velocities would meanwhile cause faster cooling rates for the deposited molecules and destabilize the sample. The competition between the two factors results in a remarkable nonmonotonic variation of the sample's stability where an optimal velocity can be quantitatively resolved. Implications of our findings for better controlling molecular-level mechanisms in glassy materials are discussed.
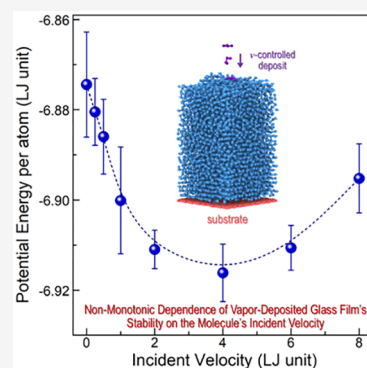
INTRODUCTION

Glasses, as amorphous and kinetically arrested metastable systems, provide ample opportunities for property control. For example, due to disordered atomic packing, the composition window of single-phase glasses can be rather broad, offering much higher flexibility compared with their crystalline counterparts.[1,2] Moreover, the nonequilibrium nature of vitrification kinetics ensures a wide range of processing routes to tune the glassy states with diverse properties.[3−6] These features have endowed glasses with promising potential in many applications, including organic electronics,[7] amorphous pharmaceuticals,[8,9] coatings for wear protection,[10] etc.

In the past decade, the physical vapor deposition (PVD)-synthesized glasses have drawn significant attention because, compared with the conventional liquid-cooling protocol, PVD can remarkably improve the glasses' stability by 4−5 orders of magnitude,[7,11] which is desirable for many technological purposes.[12,13] A wide spectrum of techniques, including both experiment and computational modeling, have been employed to unravel the novel features of PVD glasses, including the surface diffusion effect,[14] tail segregation effect,[15] interatomic potential effect,[16] molecular orientation effect,[17] etc. Among all of those studies, tremendous efforts have been made toward identifying the key parameters in PVD and elucidating their influences on the stability of deposited glasses.[3,7,8,10,11,18,19] For instance, the samples prepared at slower deposition rates are at deeper energy levels (i.e., more stable) than those produced at faster deposition rates.[1,11,20] The substrate temperature (T_s) has also been shown to play a critical role, and there exists an optimal T_s[3,8,19] that can most effectively stabilize the deposited samples.

Recent studies[3] indicate that the surface impact triggered by incident hot molecules might further relax the glassy film. However, a fundamental and predictive knowledge of the underlying mechanism of such relaxation remains elusive. In the present study, we restrict our scope to the role of the incident velocity of the deposited molecules in PVD, with a particular focus on how it could affect the sample's stability, and how it would interplay with other operating parameters. By examining the surface atoms' space−time correlations, as well as the morphology development of the film's growth front, the dual role of incident velocity is discovered. On one hand, a faster impact speed would impose the surface atoms into an effectively higher-temperature environment, which could facilitate the relaxation of the sample as it approaches the glass transition temperature (T_g). On the other hand, a higher velocity would meanwhile cause a larger cooling rate for the deposited hot molecules, which instead would destabilize the system. The competition between the two factors results in a nonmonotonic dependence of the sample's stability on the incident velocity, and an optimal condition is thus derived. Such a newly discovered mechanism, together with the existing knowledge on the deposition rate and substrate temperature
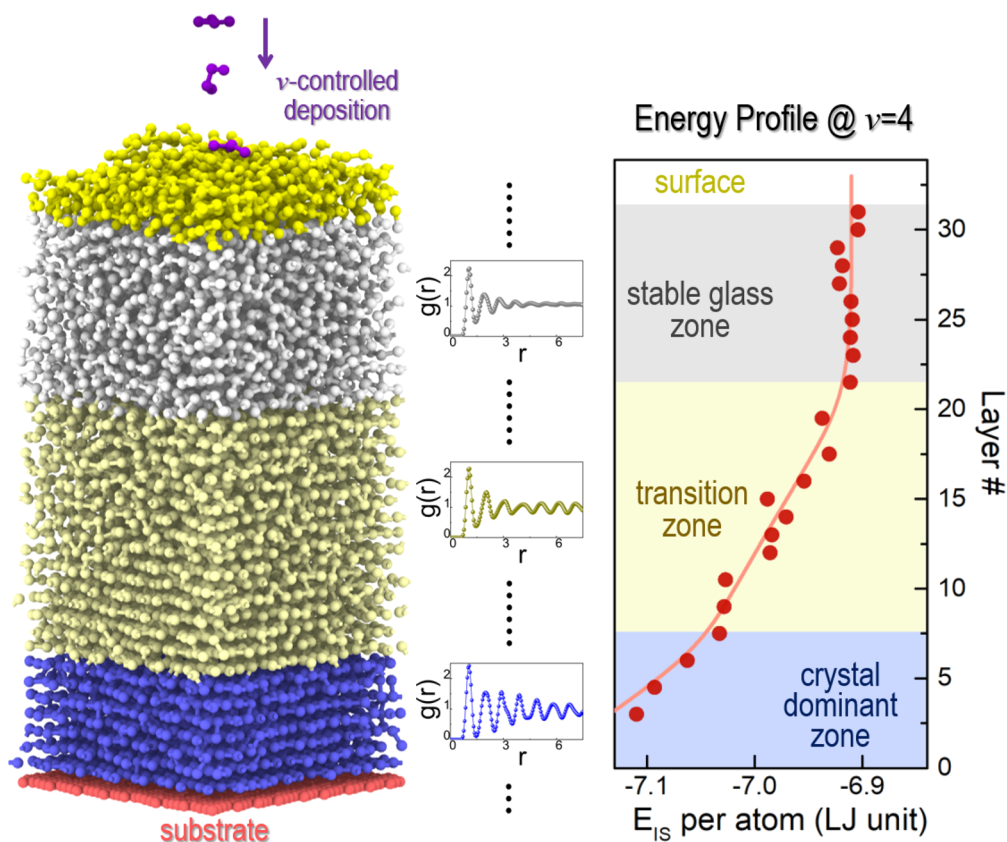
Figure 1. (Left) Illustration of v-controlled PVD modeling with $N = 4$ polymer chains. The microstructure of the deposited film is heterogeneous, gradually changing from a crystalline structure to an amorphous structure, as reflected in the distinct radial distribution functions along the normal direction. (Right) Variation of inherent structure energy (E_{IS}) along the normal direction at $v = 4$. All the calculations and discussions below are based on the properties of a stable glass zone at various net incident velocities.

effects, could potentially enable a better control on the properties of PVD glasses.

METHODS

Herein we consider a bead−spring polymer model[11,21] whose glass-forming behaviors in both the bulk and surface have been exhaustively examined.[11,18,21,22] Neighboring beads (i.e., monomers) in the same chain are connected by springs with the strength of $U_b = 1000(r - 0.97)^2$. In addition, all particles (both monomers (M) and substrate (S) atoms) also interact through a pairwise Lennard-Jones (LJ) potential with the parameters $\epsilon_{MM} = 1.0$, $\sigma_{MM} = 1.0$, $\epsilon_{MS} = 1.0$, $\sigma_{MS} = 1.0$, $\epsilon_{SS} = 0.1$, $\sigma_{SS} = 0.6$, and $r_{cut} = 2.5$. All the variables in this work are in LJ units.

The substrate was prepared by first distributing 800 S atoms into a $15 \times 15 \times 1$ thin layer at the bottom of the simulation box in an fcc (111) planar structure.[21] Then, a minimization was followed, and the atoms were finally constrained to their present positions within a strong harmonic potential well with a spring constant of 1000.[21] Periodic boundary conditions were applied along the x- and y-directions, while a fixed boundary condition was applied in the z-direction.

To replicate the PVD processes, hot polymer chains ($T = 1.0$) are deposited onto the surface in a sequential manner, specifically, each time a new chain is introduced in the vacuum above the surface with a random lateral coordinate. To probe the incident velocity effect, a controlled net velocity is applied to the mass center of the chain along the $-z$ direction ranging from $v = 0$ to $v = 8$. Note that the $v = 0$ condition does not

mean the polymer chain is static or frozen in space. It only means that the net velocity of the chain's mass center is zero, while the individual atoms in each molecule chain still have significant mobility because of the high-temperature thermalization at $T = 1.0$. After the hot chain is in contact with the surface, an MD relaxation at the length of 1000 time steps is employed, during which the substrate is kept at a lower temperature of $T_s = 0.3$ using the Nose−Hoover thermostat. Finally, the chain is cooled to T_s under a controlled time period, t_d, and the deposition rate is thus denoted as $q_d = 1/t_d$.[11] The stability of the formed glass layer is then quantified by its inherent structure (IS) energy, E_{IS}, through an energy minimization calculation. Not only is this because E_{IS} has been observed as an effective stability indicator of PVD glasses,[18] but also the correlations between various ISs in the system's underlying potential energy landscape could provide deep insights into the properties of generally disordered and nonequilibrium materials.[23,24] Note that, to restrict the scope of the present study to an incident velocity effect, we selected a short polymer chain ($N = 4$) to avoid other complex factors such as entanglement.[18,25]

RESULTS AND DISCUSSION

Figure 1 shows the representative film deposited at the conditions of $v = 4$ and $q_d = 1/750$. The microstructure of the film is clearly nonhomogeneous, as reflected in the distinct radial distribution functions along the normal direction. The polymer chains near the bottom (blue regime) maintain a long-range order, which is inherited from the substrate. At a

larger height (light yellow regime), more disorders start to build in, and the polymer chains are gradually transitioning to amorphous structures, accompanied by the consistent increase of E_{IS}. Eventually, in the light gray regime, a uniform glass phase is formed, and E_{IS} converges to a constant level. Unless otherwise noted, all the calculations and discussions in the present work are based on the properties of such a stable glass regime.

Figure 2 shows the E_{IS} of the polymer glasses at different incident velocities while keeping the same deposition rate (q_d =
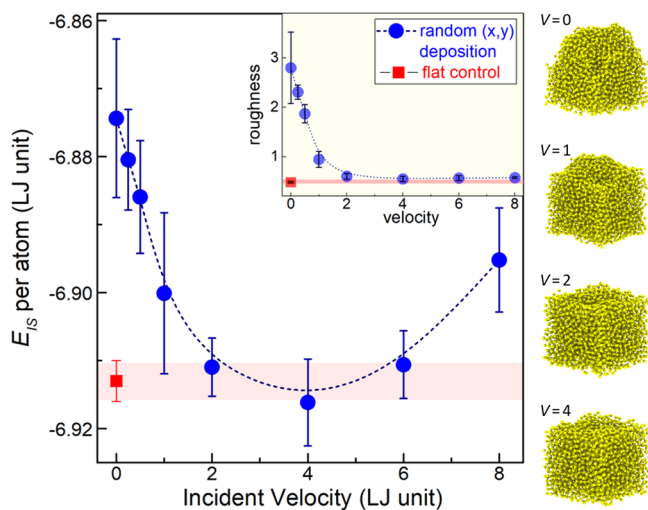
Figure 2. Blue circles in the main plot represent the E_{IS} of the deposited polymer glasses at different incident velocities while keeping the same deposition rate at q_d = 1/750. The inset plot shows the velocity effect on the surface roughness, which is defined as $R = \langle (Z_{ij} - \bar{Z})^2 \rangle^{1/2}$, where the xy plane is divided into a 15 × 15 grid and Z_{ij} represents the highest z-coordinate in each square. Four representative surface configurations at different incident velocities are shown in the right column. The red squares in the plots are the contrast results under a flat-control protocol where the newly deposited polymer chain is always placed right above the global minimum of the present surface with *zero-net velocity*.

1/750). It can be seen that, compared with the $v = 0$ cases that have been employed in earlier studies,[1,11,18] the finite incident velocity could further enhance the stability of the sample. More detailed analysis (Figure S1 in Supporting Information) shows that the production efficiency of PVD glasses can be enhanced by up to 10 times with such v-controlled deposition. More importantly, an evident nonmonotonic effect is observed: as velocity increases, the E_{IS} will first decrease, reaching an optimal value at $v = 4$, and then it starts to increase instead. The density of a sample has been hypothesized to correlate with its stability.[1,8] However, no such connection is observed in the present study (Figure S2 in Supporting Information), suggesting that the hereby observed nonmonotonic behavior is determined by alternative mechanisms that will be discussed below.

By examining the morphology of the film's growth front, we discover a qualitative distinction from low-v to high-v depositions. To be more specific, at a low incident velocity the newly deposited chain can be easily attracted and tethered to the existing high rises on the surface (Movie S1); by contrast, at increased v, the larger kinetic energy enables a higher chance for the chain to escape from the local trap near

the initial contact zone (Movie S2) and thus to explore a vaster area both in real space and in phase space of the potential energy landscape (PEL). This explains the structural and energetic variation in the early stage $v \in [0, 2]$ seen in Figure 2, namely, the smoother surface and lower E_{IS} at increasing v. To further validate such a picture, a contrast flat-control deposition at $v = 0$ has been employed. Instead of imposing a random lateral coordinate, now the polymer chain is placed right above the global minimum of the present surface to ensure a flat growth front. The obtained E_{IS} and surface roughness of the flat-control sample are marked in the main plot, and the inset plot, respectively. The results are comparable with that in the $v = 2$ case, suggesting that the stability variations from $v = 0$ to $v = 2$ can indeed be attributed to the competition between a surface trap and kinetic escape. However, as shown by the inset plot in Figure 2, the surface roughness converges to a constant level when $v > 2$, indicating the E_{IS} variation in the regime $v \in [2, 8]$ is governed by other mechanisms.
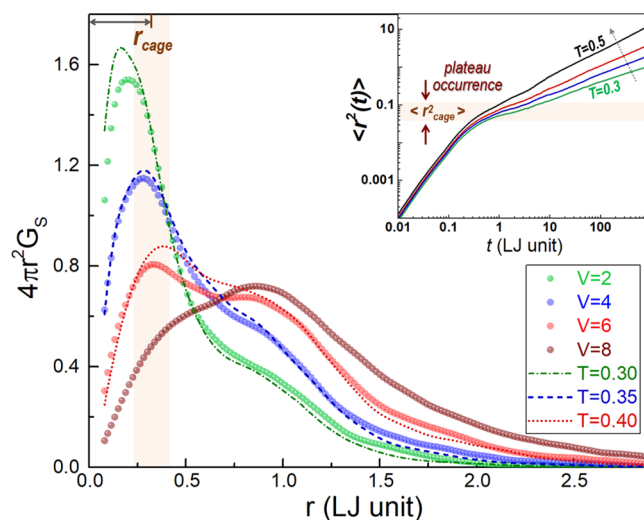
Figure 3. Self-part of the van Hove correlation function of the surface-layer atoms during PVD processing at different incident velocities (Δt = 87 500). The dashed lines are the reference curves under the normal thermal control at various temperatures. All the results are the averages of 15 independent cases. Inset plot shows the mean square displacement (MSD) curves, from which the cage size can be estimated according to the occurrence of the plateau (details in Figure S4 in Supporting Information.).

In Figure 3, we examine the particles' space−time correlations by calculating the self-part of the van Hove function[26−28] defined as

$$G_S(\mathbf{r}, \Delta t) = \frac{1}{N_{top}} \left\langle \sum_{i=1}^{N_{top}} \delta(\mathbf{r} + \mathbf{r}_i(0) - \mathbf{r}_i(\Delta t)) \right\rangle \tag{1}$$

where only top-layer particles (N_{top}) are considered because the mobilities of sublayer molecules are substantially suppressed as the deposited film grows in thickness[3,29] (Figure S3 in Supporting Information). For a similar consideration, Δt in eq 1 is set as 87 500 time steps, which corresponds to the time when all the present surface particles will be buried under a newly deposited layer.
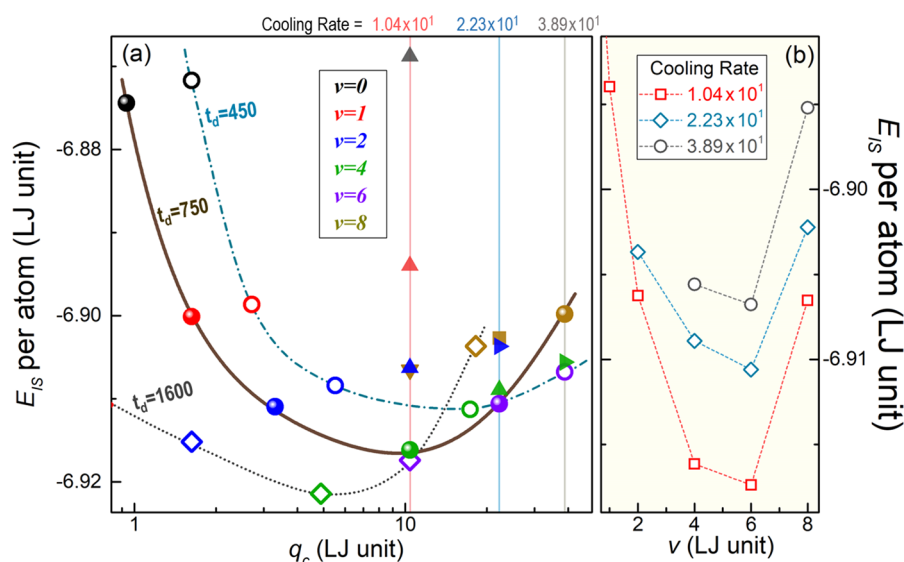
Figure 4. (a) E_{IS} of PVD-prepared polymer glasses at various conditions of incident velocities, deposition rates, and effective cooling rates. (b) Variation of E_{IS} as a function of incident velocity under controlled cooling rates.

The calculated $G_s(\mathbf{r}, t)$ values at different incident velocities are shown by the scattered data points in Figure 3. It can be seen that the distribution profile gradually shifts toward the larger r direction at increasing v. This is not surprising, because the incident chain at a higher velocity could transfer more kinetic energy and momentum to existing surface atoms. It would impose effectively a higher environmental temperature to the top-layer particles, and their mobilities are therefore enhanced. For example, according to the reference curves in Figure 3, when v increases from 2 to 4 the effective temperature changes from 0.3 (i.e., T_s) to about 0.35.

It is worth noting that, for the cases at $v = 2$ and $v = 4$, the $G_s(\mathbf{r}, t)$ profiles show a very clear single-peak structure with the maximum positions at 0.2–0.25. These are smaller than the cage size of this system estimated to be at 0.33 ± 0.09 (Figure S4 in Supporting Information), suggesting that the particles exhibit a cage-rattling dynamics mode. On the other hand, when the incident velocity reaches $v = 6$, a second mode around $r = 1.0$ starts to emerge, indicating that the system is approaching the glass transition.[22,27,28,30] The contrast with the red reference curve in Figure 3 suggests that T_g for the surface layer is slightly lower than 0.4. With a further increase in the velocity to $v = 8$, the first peak disappears, meaning the particles are no longer confined in the cage. In other words, the system is driven from a glassy state to a supercooled liquid state. As a result, a thermal rejuvenation process is taking place in this regime, which explains the significant E_{IS} increase from $v = 6$ to $v = 8$ in Figure 2.

In what follows, we restrict our attention to probe the underlying mechanism of the nonmonotonic energy variation in the range $2 \leq v \leq 6$ and to explain why the optimal velocity occurs at $v = 4$.

As an inherently nonequilibrium state of matter, glassy materials' properties are largely dependent on their processing histories.[1,5−7,22] For example, the quench rate is a key parameter in conventional liquid-cooling syntheses, and a slower quench rates can provide the sample with an enhanced stability. However, the quench rate is no longer an independent control parameter in the PVD processing which is the focus of the present study. More specifically, the effective

cooling rate of the deposited hot chain is coupled with the deposition time t_d, and the incident velocity, v:

$$q_c = \frac{T_{eff} - T_s}{t_d} = q_d[T_{eff}(v) - T_s] \tag{2}$$

where T_{eff} represents the effective temperature of the deposited chain that is determined by its incident velocity v, while t_d represents the deposition time discussed earlier when the hot chain is cooled to the substrate temperature T_s. It is clear from eq 2 that a faster v will lead to a larger q_c while the other parameters remain fixed.

Figure 4a shows the E_{IS} of the glass layers under various PVD conditions. For the convenience of interpreting the results, the data points with the same velocity are assigned with the same color noted in the legend, while the data points with the same t_d (i.e., the same deposition rate q_d) are connected by different curves marked in the plot.

Two important features embedded in Figure 4 are worth noting: (i) At first, as seen by the same-colored data points in Figure 4a, when the velocity is fixed, a faster cooling rate always leads to a less stable (i.e., higher energy) state, which is consistent with the conventional wisdom.[1,3,5,22] (ii) Second, if one compares the data points along the same vertical grid line (i.e., at fixed cooling rate), then the most stable samples always occur at $v = 6$, as seen in Figure 4b. Such behavior is consistent with the results shown in Figure 3; namely, the deposition at $v = 6$ would impose the surface atoms effectively into a sub-T_g environment, which is known to have the ability to most efficiently stabilize a glassy system.[31]

We would like to remark that these two features with the opposite trends constitute the nonmonotonic E_{IS} variations at fixed t_d conditions seen in both Figures 4a and 2. More specifically, we consider as one increases the incident velocity in the regime $v \in [2, 6]$ under a controlled t_d: on one hand, it will drive the system to approach to the T_g and thus stabilize the sample, while on the other hand, a higher v would increase the cooling rate, which would reduce the stability instead. As a result, an optimal velocity is expected to exist, and as shown by the three t_d-control curves in Figure 4a the optimal position is

around $v = 4$ (at least in the present parameter space, $450 \leq t_d \leq 1600$), which explains the energy minimum in Figure 2.

CONCLUSIONS

In summary, the present study investigated the role of molecules' incident velocity in PVD. It is observed that the stability of deposited glassy samples can be notably enhanced comparing with those prepared at zero-net velocity deposition (i.e., $v = 0$) in earlier simulations.[1,11,18] We further demonstrated that the influence of incident velocity can be characterized in three distinct regimes: (i) In the low-velocity regime $v \in [0, 2]$, by increasing v the larger kinetic energy provides the deposited molecule with a higher escaping probability from the initial trap, allowing it to explore a vaster area both in real space and in PEL space and thus to reach to a lower E_{IS} state. (ii) An inverse correlation takes place in the high-velocity condition $v \in [6, 8]$, because in this regime increasing v makes the surface molecules driven from a glassy state to a supercooled liquid state, which leads to a higher E_{IS} state due to the thermal rejuvenation process. (iii) In the intermediate regime $v \in [2, 6]$, the strong coupling between v, t_d, and q_c leads to a remarkable nonmonotonic variation of E_{IS}. Specifically, an increased v will drive the particles to a sub-T_g environment that would stabilize the sample, but on the other hand, it will also cause a faster cooling rate that instead would reduce the stability.

We hope that the novel roles of incident velocity discovered in the present study, as well as the obtained optimal conditions, will stimulate future experimental validations. For example, compared with thermal evaporation, the e-beam assisted PVD can effectively control the incidental direction of the arriving atoms. The momentum distribution of deposited particles can also be controlled by tuning the plasma pressure in magnetron sputtering deposition. Specifically, at low pressure there are only a few collisions in the plasma, and the particles can be deposited at a well-defined direction; on the contrary, at high pressure the large amount of collisions in the plasma would lead to a nearly thermalized distribution of incident particles. In our simulation, $v = 0$ corresponds to a pure thermalized scenario, while $v > 0$ represents a more directed deposition. Therefore, the present study (e.g., Figure 2) can possibly be examined by the above-mentioned experimental techniques, which might potentially facilitate exploiting the PVD design/processing space and identifying optimized routes to prepare molecule glasses or even metallic glasses[4,32] with unprecedented properties. Admittedly, there are new questions remaining to be answered. For example, recent studies[3] demonstrate that the ideal substrate temperature T_s is dependent on the deposition rate $1/t_d$. Therefore, given the identified coupling effect between v and t_d in the present study, there is reason to also expect a strong interplay of incident velocity and T_s, which would warrant further studies.

ASSOCIATED CONTENT

ⓈⒾ Supporting Information

The Supporting Information is available free of charge at https://pubs.acs.org/doi/10.1021/acs.jpcb.0c02335.

> Details about the relative stability of differently prepared glasses, the relationship between stability and density, the self-part of van Hove correlation function of the surface and subsurface particles, and the caging effect and the cage size (PDF)
>
> Movie showing the effect of chain mobility on surface roughness under low-velocity scenario (MP4)
>
> Movie showing the effect of chain mobility on surface roughness under high-velocity scenario (MP4)

AUTHOR INFORMATION

Corresponding Author
Yue Fan − *Department of Mechanical Engineering, University of Michigan, Ann Arbor, Michigan 48109, United States;* ⓘ orcid.org/0000-0001-6558-3970; Email: fanyue@umich.edu

Author
Yuchu Wang − *Department of Mechanical Engineering, University of Michigan, Ann Arbor, Michigan 48109, United States*

Complete contact information is available at:
https://pubs.acs.org/10.1021/acs.jpcb.0c02335

Notes
The authors declare no competing financial interest.

REFERENCES

(1) Singh, S.; Ediger, M. D.; De Pablo, J. J. Ultrastable glasses from in silico vapour deposition. *Nat. Mater.* **2013**, *12*, 139−144.

(2) Berthier, L.; Ediger, M. Facets of glass physics. *Phys. Today* **2016**, *69*, 40.

(3) Reid, D. R.; Lyubimov, I.; Ediger, M.; De Pablo, J. J. Age and structure of a model vapour-deposited glass. *Nat. Commun.* **2016**, *7*, 13062.

(4) Luo, P.; Cao, C.; Zhu, F.; Lv, Y.; Liu, Y.; Wen, P.; Bai, H.; Vaughan, G.; di Michiel, M.; Ruta, B.; et al. Ultrastable metallic glasses formed on cold substrates. *Nat. Commun.* **2018**, *9*, 1389.

(5) Debenedetti, P. G.; Stillinger, F. H. Supercooled liquids and the glass transition. *Nature* **2001**, *410*, 259−267.

(6) Dyre, J. C. Colloquium: The glass transition and elastic models of glass-forming liquids. *Rev. Mod. Phys.* **2006**, *78*, 953.

(7) Ediger, M. D. Perspective: Highly stable vapor-deposited glasses. *J. Chem. Phys.* **2017**, *147*, 210901.

(8) Swallen, S. F.; Kearns, K. L.; Mapes, M. K.; Kim, Y. S.; McMahon, R. J.; Ediger, M. D.; Wu, T.; Yu, L.; Satija, S. Organic glasses with exceptional thermodynamic and kinetic stability. *Science* **2007**, *315*, 353−356.

(9) Yu, L. Amorphous pharmaceutical solids: preparation, characterization and stabilization. *Adv. Drug Delivery Rev.* **2001**, *48*, 27−42.

(10) Yu, H.-B.; Luo, Y.; Samwer, K. Ultrastable metallic glass. *Adv. Mater.* **2013**, *25*, 5904−5908.

(11) Lin, P.-H.; Lyubimov, I.; Yu, L.; Ediger, M.; de Pablo, J. J. Molecular modeling of vapor-deposited polymer glasses. *J. Chem. Phys.* **2014**, *140*, 204504.

(12) Ediger, M. Vapor-deposited glasses provide clearer view of two-level systems. *Proc. Natl. Acad. Sci. U. S. A.* **2014**, *111*, 11232−11233.

(13) Pérez-Castañeda, T.; Rodríguez-Tinoco, C.; Rodríguez-Viejo, J.; Ramos, M. A. Suppression of tunneling two-level systems in ultrastable glasses of indomethacin. *Proc. Natl. Acad. Sci. U. S. A.* **2014**, *111*, 11275−11280.

(14) Zhu, L.; Brian, C.; Swallen, S.; Straus, P.; Ediger, M.; Yu, L. Surface self-diffusion of an organic glass. *Phys. Rev. Lett.* **2011**, *106*, 256103.

(15) Moore, A. R.; Huang, G.; Wolf, S.; Walsh, P. J.; Fakhraai, Z.; Riggleman, R. A. Effects of microstructure formation on the stability of vapor-deposited glasses. *Proc. Natl. Acad. Sci. U. S. A.* **2019**, *116*, 5937−5942.

(16) Friederich, P.; Rodin, V.; von Wrochem, F.; Wenzel, W. Built-in potentials induced by molecular order in amorphous organic thin films. *ACS Appl. Mater. Interfaces* **2018**, *10*, 1881−1887.

(17) Youn, Y.; Yoo, D.; Song, H.; Kang, Y.; Kim, K. Y.; Jeon, S. H.; Cho, Y.; Chae, K.; Han, S. All-atom simulation of molecular orientation in vapor-deposited organic light-emitting diodes. *J. Mater. Chem. C* **2018**, *6*, 1015−1022.

(18) Helfferich, J.; Lyubimov, I.; Reid, D.; de Pablo, J. J. Inherent structure energy is a good indicator of molecular mobility in glasses. *Soft Matter* **2016**, *12*, 5898−5904.

(19) Kearns, K. L.; Swallen, S. F.; Ediger, M.; Wu, T.; Yu, L. Influence of substrate temperature on the stability of glasses prepared by vapor deposition. *J. Chem. Phys.* **2007**, *127*, 154702.

(20) Kearns, K. L.; Swallen, S. F.; Ediger, M. D.; Wu, T.; Sun, Y.; Yu, L. Hiking down the energy landscape: Progress toward the Kauzmann temperature via vapor deposition. *J. Phys. Chem. B* **2008**, *112*, 4934−4942.

(21) Singh, S.; de Pablo, J. J. A molecular view of vapor deposited glasses. *J. Chem. Phys.* **2011**, *134*, 194903.

(22) Barrat, J.-L.; Baschnagel, J.; Lyulin, A. Molecular dynamics simulations of glassy polymers. *Soft Matter* **2010**, *6*, 3430−3446.

(23) Liu, C.; Guan, P.; Fan, Y. Correlating defects density in metallic glasses with the distribution of inherent structures in potential energy landscape. *Acta Mater.* **2018**, *161*, 295−301.

(24) Fan, Y.; Yildiz, B.; Yip, S. Analogy between glass rheology and crystal plasticity: Yielding at high strain rate. *Soft Matter* **2013**, *9*, 9511−9514.

(25) Everaers, R.; Sukumaran, S. K.; Grest, G. S.; Svaneborg, C.; Sivasubramanian, A.; Kremer, K. Rheology and microscopic topology of entangled polymeric liquids. *Science* **2004**, *303*, 823−826.

(26) Scheidler, P.; Kob, W.; Binder, K. The relaxation dynamics of a supercooled liquid confined by rough walls. *J. Phys. Chem. B* **2004**, *108*, 6673−6686.

(27) Peter, S.; Meyer, H.; Baschnagel, J. MD simulation of concentrated polymer solutions: Structural relaxation near the glass transition. *Eur. Phys. J. E: Soft Matter Biol. Phys.* **2009**, *28*, 147−158.

(28) Jaiswal, A.; Egami, T.; Zhang, Y. Atomic-scale dynamics of a model glass-forming metallic liquid: Dynamical crossover, dynamical decoupling, and dynamical clustering. *Phys. Rev. B: Condens. Matter Mater. Phys.* **2015**, *91*, 134204.

(29) Lyubimov, I.; Antony, L.; Walters, D. M.; Rodney, D.; Ediger, M.; de Pablo, J. J. Orientational anisotropy in simulated vapor-deposited molecular glasses. *J. Chem. Phys.* **2015**, *143*, 094502.

(30) Stillinger, F. H.; Debenedetti, P. G. Glass transition thermodynamics and kinetics. *Annu. Rev. Condens. Matter Phys.* **2013**, *4*, 263−285.

(31) Zhang, F.; Mendelev, M. I.; Zhang, Y.; Wang, C.-Z.; Kramer, M. J.; Ho, K.-M. Effects of sub-Tg annealing on Cu64. 5Zr35. 5 glasses: A molecular dynamics study. *Appl. Phys. Lett.* **2014**, *104*, 061905.

(32) Bokas, G.; Zhao, L.; Morgan, D.; Szlufarska, I. Increased stability of CuZrAl metallic glasses prepared by physical vapor deposition. *J. Alloys Compd.* **2017**, *728*, 1110−1115.